AN EFFICIENT IMAGE DEHAZING FOR ACCURATE OBJECT DETECTION

ERAY KAÇMAZ

Thesis for the Master's Program in Computer Engineering

Graduate School

Izmir University of Economics

Izmir

2023

AN EFFICIENT IMAGE DEHAZING FOR ACCURATE OBJECT DETECTION

ERAY KAÇMAZ

ADVISOR: ASSOC. PROF. DR. MEHMET TÜRKAN

CO-ADVISOR: ASSOC. PROF. DR. KAYA OĞUZ

A Master's Thesis

Submitted to

the Graduate School of Izmir University of Economics

the Department of Computer Engineering

Izmir

2023

ETHICAL DECLARATION

I hereby declare that I am the sole author of this thesis and that I have conducted my work in accordance with academic rules and ethical behavior at every stage from the planning of the thesis to its defense. I confirm that I have cited all ideas, information and findings that are not specific to my study, as required by the code of ethical behavior, and that all statements not cited are my own.

Name, Surname:
Eray KAÇMAZ
Date:
07.07.2023
Signature:

ABSTRACT

AN EFFICIENT IMAGE DEHAZING FOR ACCURATE OBJECT DETECTION

KAÇMAZ**,** Eray

Master's Program in Computer Engineering

Advisor: Assoc. Prof. Dr. Mehmet TÜRKAN

Co-Advisor: Assoc. Prof. Dr. Kaya OĞUZ

July, 2023

The weather phenomenon known as “haze” significantly reduces the ability to see external scenery. The light-absorbing and light-scattering particulates mainly bring this on in the atmosphere. This thesis suggests a single image fusion-based dehazing method for precise object identification. To apply the fusion process, weight maps are computed for each RGB layer of each image using a collection of gamma-corrected images. To generate more accurate results, the combination of the Laplacian pyramid for inputs and the Gaussian pyramid for weight maps is used in the fusion process. Hazy input and final output images are tested in the YOLOv7 algorithm to detect objects accurately. Comprehensive tests are conducted to compare the proposed method with the other approaches. The experimental results on a range of hazy pictures demonstrate the prior's strength both visually and quantitatively, showcasing the superiority of the developed algorithm over several cutting-edge methods in the literature.

Keywords: Image Dehazing, Object Detection, Weight Map Extraction.

ÖZET

HASSAS NESNE TANIMA İÇİN ETKİLİ BİR GÖRÜNTÜ SİS GIDERME YÖNTEMİ

KAÇMAZ**,** Eray

Bilgisayar Mühendisliği Yüksek Lisans Programı

Tez Danışmanı: Doç. Dr. Mehmet TÜRKAN

İkinci Tez Danışmanı: Doç. Dr. Kaya OĞUZ

Temmuz, 2023

Hava olayı olarak bilinen “sis”, dış manzarayı görme yeteneğini önemli ölçüde azaltır. Atmosferdeki ışığı emen ve ışığı saçan partiküller bunun başlıca nedenidir. Bu tez çalışması, hassas nesne tanımama için görüntü birleştirme tabanlı bir sis giderme yöntemi sunmaktadır. Birleştirme sürecini uygulamak için, her görüntünün her RGB katmanı için ağırlık haritaları, gama düzeltmesi yapılmış görüntüler kullanılarak hesaplanmaktadır. Daha doğru sonuçlar elde etmek için, füzyon işleminde girdiler için Laplace piramidi ve ağırlık haritaları için Gauss piramidi kombinasyonu kullanılmaktadır. Sisli girdi ve nihai çıktı görüntüleri, nesneleri doğru bir şekilde tespit etmek için YOLOv7 algoritmasında test edilmektedir. Geliştirilen yöntemi diğer yaklaşımlarla karşılaştırmak için kapsamlı testler yapılmıştır. Çeşitli sisli görüntüler üzerine sunulan sonuçlar, önerilen algoritmanın etkinliğini hem görsel hem de nicel olarak değerlendirerek yöntemin literatürdeki birçok öncü yönteme göre üstünlüğü

sergilenmektedir.

Anahtar Kelimeler: Sis Giderme, Nesne Tanıma, Ağırlık Haritaları Çıkarma.

To my eternal loves, my daughter and wife

ACKNOWLEDGEMENTS

I would like to express my greatest appreciation to my supervisor, Assoc. Prof. Dr. Mehmet TÜRKAN for his continuous support, supreme supervision, motivation, and constructive comments throughout my graduate studies. I feel very fortunate to become his student; thanks to his guidance I have improved myself considerably for the aims I am pursuing.

I would like to extend my sincere appreciation to my co-advisor, Assoc. Prof. Dr. Kaya OĞUZ, for his invaluable contributions to my academic journey. His guidance and the Machine Learning course he offered have been instrumental in sparking my interest and leading me to pursue research in the captivating fields of AI and Image Processing. I am truly grateful for his support, mentorship, and for connecting me with valuable opportunities.

I would like to express my sincere appreciation to TÜBİTAK for their support through the 2210-A General Domestic Graduate Scholarship Program. Their support has played a vital role in the completion of this thesis.

I would also like to express my heartfelt appreciation to my loving wife and daughter, whose unwavering support and understanding have been crucial during my graduate studies. Their patience, encouragement, and belief in my abilities have been a constant source of strength and motivation.

TABLE OF CONTENTS

LIST OF TABLES

LIST OF FIGURES

LIST OF ABBREVIATIONS

BRISQUE: Blind/Referenceless Image Spatial Quality Evaluator

CLAHE: Contrast Limited Adaptive Histogram Equalization

CNN: Convolutional Neural Network

DCP: Dark Channel Prior

IQA: Image Quality Assessment

MEF: Multi-Exposure Fusion

PIQE: Perception based Image Quality Evaluator

PSNR: Peak Signal-to-Noise Ratio

SSIM: Structural Similarity Index Measure

WM: Weight Map

CHAPTER 1: INTRODUCTION

In the presence of specific physical occurrences, such as mist, haze or fog, tiny airborne particles make it harder to see an exterior scene. Haze in images is a common issue in various fields, such as computer vision, photography, and remote sensing. Hazy images suffer from low contrast, whitened tone, and color fading, degrading image quality and hindering the efficiency of vision algorithms. Furthermore, the existence of atmospheric haze can pose significant challenges to safety-critical systems, such as autonomous vehicles, where accurate object detection and recognition are vital. In recent years, image dehazing techniques have been widely studied to address this issue. Recovering the original appearance of a hazy image by removing unwanted visual effects caused by haze is the primary objective of dehazing algorithms.

Dehazing is considerably asked for in computer vision and photography applications due to its ability to significantly improve the scene's clarity and adjust the color change brought on by the atmospheric light. By removing haze, clarity of the scene can be significantly enhanced, and the undesired color shifts caused by atmospheric light can be corrected. This restoration of a haze-free image typically results in improved visual aesthetics.

Moreover, most computer vision algorithms, both high-level object identification and low-level picture analysis, presume that the incoming image represents the scene's radiance. However, haze introduces distortions and reduces contrast in the captured scene, thereby inevitably hindering the performance of numerous vision algorithms.

Efforts to address challenges imposed by haze have led to comprehensive research and the advancement of image dehazing techniques. Dehazing aims to recover the original appearance of a hazy image by reducing or eliminating the visual artifacts induced by atmospheric haze. Numerous dehazing algorithms have been proposed, employing various methodologies such as image priors, atmospheric scattering models, and machine learning-based approaches. These techniques enhance image quality, restore accurate color information, and improve the visibility of objects and details within hazy scenes.

Despite significant progress in the field of image dehazing, there are still areas that still need further exploration. Another vital aspect that necessitates attention is the development of efficient and real-time dehazing algorithms, especially for safety-critical systems like autonomous vehicles. The accurate detection and recognition of objects in hazy conditions are crucial for ensuring the reliability and effectiveness of autonomous driving systems. Therefore, the integration of dehazing techniques with object detection algorithms becomes essential to overcome the challenges introduced by atmospheric haze. Addressing these issues aims to advance the field of image dehazing and enable the development of robust vision systems capable of performing effectively in various real-world scenarios affected by haze and other adverse atmospheric conditions.

Image dehazing is a technique used to eliminate unwanted haze-related visual impacts and improve the clarity of images taken in severe atmospheric environments. Dehazing the picture aims to improve scene clarity so that essential data can be captured. In the past few decades, a diverse array of techniques for removing haze has been extensively explored and proposed in the existing literature. In the rapidly advancing field of image processing, Wang et al. (2017), Babu et al. (2020), and Agrawal et al. (2022) have conducted comprehensive reviews aiming to making comparisons among various state-of-the-art haze removal methods. Their insightful studies shed light on the advancements made in the research area of haze removal techniques over the past few decades. Researchers categorized the dehazing methods in many ways with different limitations.

Techniques are classified into two main groups that are single and multiple image dehazing, based on the input image quantity. The multi-image dehazing technique utilizes methods based on polarization to recover depth-related data using different images. Using the unique properties of polarized light, these methods can improve visibility and recover the scene's depth that is obscured due to haze. These techniques restore accurate depth information by analyzing the polarization patterns in multiple images, resulting in clearer visuals. It is important to understand that polarization-based methods for multiple-image dehazing have some limitations. These methods are mainly not suitable for real-time applications due to their high computational

complexity. Also, capturing the required polarization information may require specialized equipment, which can restrict this approach's practicality and widespread adoption in certain situations.

Single-image dehazing methods, on the other hand, typically require two primary components: the ambient light caused by atmospheric conditions and the transmission map. Tan et al. (2008), Fattal (2008), and He et al. (2009) presented single-image haze removal methods that use the scene's physical characteristics to achieve this.

New techniques based on deep learning have emerged to surpass the constraints of conventional methods and enhance image dehazing. A novel approach that merges the strengths of both conventional methods and deep learning to remove unwanted visual effects caused by haze is presented in this thesis study. The goal of this approach is to preserve essential details and enhance image quality. The proposed method for solving the challenges of image dehazing combines traditional techniques grounded in understanding the physical properties of haze with the addition of the capabilities of deep learning models. Traditional methods rely on image priors and assumptions about the degradation caused by haze, while deep learning models excel at learning complex patterns and capturing intricate details from large datasets. This comprehensive approach offers an effective and successful solution to image dehazing.

The effectiveness of the proposed technique is evaluated on a benchmark dataset and compared against other state-of-the-art techniques using objective and subjective metrics. Outcomes demonstrate that the proposed technique surpasses alternative approaches regarding both quantitative and qualitative assessments. The proposed method additionally involves gamma correction of input images. It uses a combination of Gaussian and Laplacian pyramids for image fusion, similar to the approaches of Zhu et al. (2021), Ancuti et al.(2010), and Mertens et al.(2007).

To assess the object detection capabilities of the proposed algorithm, the widely recognized The YOLO (You Only Look Once) (Redmon et al., 2016) algorithm, which is initially introduced by Redmon et al. in 2016, is adopted. The YOLOv7 algorithm is used by Qiu et al. (2023), combined with AOD-NET, for object detection in

challenging foggy conditions and low-light traffic environments. Optimizing image defogging and image enhancement are combined with increasing picture clarity. After this phase, YOLOv7 is used for object detection. This thesis is organized as follows. Chapter 2 details the related work for the problem addressed in this study. In Chapter 3, the methodology employed in this study is described in detail, including dataset selection and evaluation metrics. Chapter 4 delves into the experimental results, analysis, and discussions, shedding light on the findings and implications of the research. Finally, Chapter 5, concludes the thesis by summarizing the key contributions, discussing the limitations, and suggesting potential avenues for future research.

CHAPTER 2: RELATED WORK

Dehazing is important in computer vision and image processing aiming to improve the visibility and clarity of images by removing unwanted haze, fog, or mist. Over the years, researchers have suggested various techniques to address this problem, and extended reviews have been conducted to shed light on this area of study (Agrawal and Jalal, 2022; Harish Babu and Venkatram, 2020; Wang and Yuan, 2017).

Methods include various techniques and approaches, such as models based on how light scatters in the atmosphere, using prior knowledge about images, optimization algorithms, and machine learning. Each approach provides unique insights and contributes to our understanding of dehazing. By continuously exploring and innovating in this field, researchers strive to reduce the impact of atmospheric conditions on images, which has practical applications in areas like surveillance, autonomous driving, and remote sensing. The collective efforts of researchers worldwide demonstrate a commitment to enhancing image quality and enabling reliable vision systems in challenging environments.

One of the earliest and widely adopted approaches for dehazing is the atmospheric scattering model-based method which has gained notable popularity for its efficacy in dehazing tasks proposed by He et al. (2009). This approach is based on the dark channel prior assumption, which states that the background of an object in a clear image usually has low values in the color channel. It estimates the transmission map using a haze imaging model, which is then utilized to recover the original scene radiance.

The approaches can be categorized into two primary classifications: non-learning and learning-based dehazing algorithms, and into six subcategories: depth estimation-based, fusion-based, enhancement-based, filtering-based, meta-heuristic techniques-based and supervised learning-based dehazing algorithms (Harish Babu and Venkatram, 2020).

2.1. Depth Estimation Based Dehazing

Most of the existing image dehazing methods are predicated on the utilization of techniques for estimating depth maps. Depth estimation-based dehazing algorithms can provide an enhanced approximation of the transmission map and can effectively remove haze from images with a clear depth structure. Initially, evaluating the image's depth involves considering certain assumptions or priors. Subsequently, the atmospheric veil and transmission map are determined using the assessed depth map. Effectiveness of depth map estimation methods depends entirely on underlying presumptions. However, stated methods commonly encounter a range of challenges, including but not limited to sky-region preservation, degradation of edges, color distortion, artifacts arising from gradient reversal, and halo artifacts.

Dark Channel Prior (DCP) (He et al., 2009) is proposed as a reliable method of calculating the transmission matrix. As a disadvantage, it requires accurate depth information, which may not be available or difficult to obtain in some cases. Also, it may result in artifacts in the dehazed images since it is sensitive to errors in depth estimation.

2.2. Fusion Based Dehazing

Image regions characterized by low light intensity and dense haze exhibit a notable degradation in visibility. Fusion-based image dehazing is a popular technique combining multiple metrics to remove haze from images effectively. The fusion-based method employs weight maps, and specific spatial functions are used for low-contrast pixels. All weight maps contribute equally to the final output of the fusion-based method. The impact of haze on objects in the image is influenced by the unstable intensity and contrast of color among pixels. Therefore, the image can undergo various contrast enhancement procedures to alleviate the impact of the haze. Fattal (2008) examines techniques that focus on enhancing contrast at a global level.

Mertens et al. (2007) introduces an approach incorporating the Laplacian decomposition technique for images and utilizing a Gaussian pyramid to generate weight maps. These weight maps capture relevant variables such as contrast and

saturation.

Ancuti et al. (2010) presented a method that employs a dual-input strategy. One input is derived by performing white balancing on hazy image, and the other is generated by deducting the average illumination value of the whole image from the original image. The authors use luminance, saliency, and chrominance weight maps to yield the final weight map by normalizing. Each input undergoes a pyramid decomposition process using the Laplacian operator at various sizes during the fusing process. A Gaussian pyramid is constructed for each adjusted weight projection similarly.

It is important to note that fusion-based dehazing methods have shown remarkable performance in removing haze from images. However, they have some limitations, such as the need for parameter tuning and their dependence on the quality of the input images. Furthermore, many fusion-based methods are computationally expensive, which can limit their suitability for real-time applications.

This kind of approach generally results in over/under-saturated images, representing a common limitation. Popular examples of image enhancement operators include white balance adjustment, histogram equalization, and gamma correction.

2.3. Enhancement Based Dehazing

Enhancement-based dehazing algorithms' primary objective is to enhance the crucial details while eliminating undesirable noise. These algorithms can significantly enrich the contrast and color of the dehazed images while relatively simple to implement. Various methods have been proposed for image enhancement, including histogram equalization (Fu et al., 2015), the Retinex method (Wang et al., 2018), and Weighted Histograms (He et al., 2016). However, these methods must be more efficient when applied to images with pronounced haze gradients or scenes exhibiting non-homogeneous haze. Moreover, enhancement-based dehazing algorithms may not effectively remove haze from images with severe haze or complex scenes.

2.4. Filtering Based Dehazing

Filtering-based dehazing algorithms are relatively simple to implement and effectively remove haze from low-contrast images. To improve the performance of the initial atmospheric veil estimation, several filters have been utilized, including the median filter (Zhang et al., 2012), the Weighted Guided Image Filter (Li et al., 2015), and the Bilateral filter (Sun et al., 2015).

However, methods based on filtering techniques face computational speed challenges, and the effectiveness of these methods heavily relies on the estimation performance of various priors. In addition to these shortcomings, the algorithm may be ineffective in removing haze from images with severe haze or complex structures and results in artifacts in the dehazed images, such as oversaturation or underexposure.

2.5. Meta-Heuristic Methods Based Dehazing

Parameter tuning is recognized as a difficult task in contemporary research and a crucial aspect of many dehazing techniques. Optimizing parameters can efficiently enrich the efficacy of existing dehazing methods. These parameters can be white balance factor, patch size, and restore value.

2.6. Supervised Learning Based Dehazing

Despite the abundance of methods proposed in the literature, most rely solely on features designed manually. Nevertheless, achieving effective and reliable restoration of hazy images remains an ongoing challenge. The consistency of the used prior determines how precise restoration-based approaches may be. These techniques might result in problems like persistent haze or the creation of unrealistic hazy illustrations in the case that the predecessor fails. As a result, researchers have recently turned to machine learning models to improve the efficiency of depth map evaluation. Supervised learning-based dehazing algorithms can provide superior dehazed images with less artifacts and are appropriate for real-time applications.

Ren et al. (2016) proposed a multi-scale CNN (MSCNN) based method that first generates a coarsely scaled transmission matrix and then progressively improves it. In addition to this, AOD-Net (Li et al., 2017) and DehazeNet (Cai et al., 2016), algorithms are evaluated as good computational speed algorithms compared with the others. DehazeNet (Cai et al., 2016) employs a deep neural network that has been trained on an extensive dataset, utilizing the ground-truth transmission maps as a reference to estimate the transmission maps.

While these learning approaches have impressive results in image dehazing, they usually require a supervised and trained approach. This means they typically need an extensive dataset with some ground truth, such as images encompassing hazy and clean versions. Without fulfilling these conditions, learning-based methods may exhibit limitations or fail to achieve desirable results.

2.7. Limitations and Future Directions of Existing Approaches

In modern research, parameter tuning is a challenging and crucial aspect of many dehazing methods. It is observed that parameters stated in *Section 2.5* can be effectively adjusted to improve the overall effectiveness of existing dehazing methods. Meta-heuristic techniques-based dehazing algorithms can effectively remove haze from images with complex structures and textures and provide good results with relatively few iterations. But as stated earlier, these algorithms may require parameter tuning. But it is a computationally expensive algorithm, which may not be appropriate for real-time applications.

It is widely recognized that each technique employed in haze removal possesses its distinct strengths and weaknesses, making it clear that no single method can be considered universally effective for all hazy images. Thus, removing haze from images continues to be a dynamic and active area of research, where scholars and experts are exploring various approaches to address this complex problem. The absence of a superior solution underscores the complex nature of haze removal and highlights the need for further investigation and innovation.

Seeking an optimal haze removal technique remains an ongoing study fueled by the endless search to enhance image quality and restore visual clarity in challenging atmospheric conditions. Through continued research efforts, advancements are expected to be made, leading to improved methodologies and a deeper understanding of the underlying mechanisms involved in haze removal.

CHAPTER 3: PROPOSED IMAGE DEHAZING ALGORITHM

Image fusion is a method used in image processing that involves collecting relevant information from multiple images and merging the collected data into a single image. Among the various image fusion techniques, multi-exposure fusion (MEF) (Burt and Adelson, 1983) is used to merge images captured at various exposures into a single, unified image. Primary purpose of MEF methods is to provide an effective solution for maintaining low dynamic range (LDR) displays and high dynamic range (HDR) image techniques compatible.

Similar to MEF, fusion-based single-image dehazing methods—the focus of this work—aim to overcome the limitations by exploiting the inherent features of a single hazy image. They have shown promising results and outperformed the majority of the dehazing techniques proposed thus far.

Fusion-based dehazing algorithms can effectively remove haze from images by combining multiple metrics and provide a flexible framework for integrating various image properties into a single weight map. This algorithm can be applied with various types of input images. Besides, it often requires parameter tuning, which can be time-consuming. Also, it can be computationally expensive.

The single-image dehazing approach proposed in this study depends on image fusion, a computational imaging area that has extensively studied and discovered many practical uses, including HDR imaging (Mertens et al., 2007). The primary concept is to merge multiple images into a single composition, keeping only the crucial elements.

The proposed image dehazing method utilizes three passes with different weight maps and input images. For the first and second passes, the method calculates the input image's mean brightness value by dividing the whole image's mean value by 255. This information is then used to derive three gamma values, which are used to expose the input image artificially. Since the haze formation always decreases the intensities of images, the input image is artificially under-exposed using γ value higher than one ($\gamma > 1$), which reduces the image's brightness. The artificially gamma-corrected outputs

of each exposure level are used as input for each pass.

The choice of the weight maps (WMs) used in each pass is based on their ability to capture different aspects of the haze and scene content. In the first pass, DCP is utilized as it can successfully remove haze from the image by estimating the haze density of the scene, providing a good starting point for subsequent passes. In the second pass, entropy and saliency complement each other, with entropy helping to improve the contrast and saliency helping to preserve the details of the scene.

The illumination-aware color correction algorithm aims to approximate the color of illumination and remove the color cast from the image. On the other hand, the gray world algorithm employs the adjustment of color balance in the image, assuming that the average color of the image should be gray. These two algorithms complement each other in removing color distortion caused by the hazy environment. Therefore, in the third pass, the proposed method uses a combination of illumination-aware color correction and gray world algorithms to create inputs for the dehazing process. The input to this last pass includes the outputs of these algorithms and the output of the second pass. The pass acts as both a post-processing and a specific object information-gathering step.

As for the additional WMs of the third pass, the log-transformed output of AlexNET's $conv1$ layer, which captures the texture information in the image, is employed. This WM is combined with the contrast WM, which captures the local contrast information, to produce the final WM. These weight maps are used to get more specific object information from the hazy area.

Overall, the proposed image dehazing method utilizes a combination of multiple passes, gamma correction, and various weight maps to enhance the effectiveness of the dehazing process. Moreover, the use of illumination-aware color correction and gray world algorithms in the third pass further enhances the color balance of the final dehazed image.

The order in which these methods are utilized is carefully chosen to ensure that the output of each pass is a good input for the subsequent pass. In the first pass, the DCP weight map is used to remove the overall haze, which can be considered a coarse-level operation since it addresses the general haziness in the image. In the second pass, the Entropy and Saliency WMs are employed as they operate at a relatively finer level by considering local contrast and saliency information. This fine-grained processing helps to refine the image and highlight important regions, improving the visibility and quality of objects. In the third pass, AlexNET's conv1 layer and contrast WMs are utilized to capture detailed information, including low-level features. By incorporating these finer WMs, the algorithm aims to enhance objects' visibility and distinctiveness, leading to improved object detection performance. In the proposed method, the order of WM choices can be considered as moving from coarse to fine.

The impacts of these four weight maps are significant in various ways, but the first one —the DCP weight map— has a more significant total effect on sight. The combined weight map W that is used in the second and third passes is produced using element-by-element multiplication using *Eq.*(*1*)*:*

$$W_n = W_n^1 \times W_n^2 \qquad (1)$$

where W_n represents the combined weight map of first WM W_n^1 and second WM W_n^2 of the $n-th$ pass. Note here that the normalization of weight maps will guarantee the total of each weight per coordinate equals one. This step is applied using *Eq.*(*2*):

$$\overline{W} = \frac{W_n}{\sum W_n} \qquad (2)$$

where $\overline{W}$ denotes the normalized WM, W_n denotes the WM of $n-th$ pass and $\sum W_n$ represents the sum of all WMs of $n-th$ pass.

The final image fusion algorithm is applied by a weighted summation as

$$J = \sum_{k=1}^{K} W_k \circ I_k \qquad (3)$$

where K denotes the number of input images, I_k represents $k-th$ input, $\circ$ denotes the element-by-element multiplication and W_k is the corresponding weight map. The fused output J indicates the fused values of pixels located in the same position within the input images.

The *Eq.*(*3*) alone yields an undesirable outcome, as visible artifacts occur wherever there are rapid weighting variations. This occurs because the merged images possess varying absolute intensities. Although a weight map smoothing via a Gaussian filter could eliminate abrupt transitions, it can also introduce unwanted halos around edges and lead to the spill of information across object boundaries.

To avoid halo artifacts, pyramidal refinement is implemented by Burt et al. (1983), and Mertens et al. (2007). This method decomposes input images into a Laplacian pyramid, whereas weight maps are into a Gaussian pyramid.

Blending is applied using *Eq.*(*4*):

$$\boldsymbol{L}\{J\}_{ij}^{l} = \sum_{k=1}^{K} \boldsymbol{G}\{W\}_{ij,k}^{l} \boldsymbol{L}\{I\}_{ij,k}^{l} \qquad (4)$$

where $\boldsymbol{L}\{J\}_{ij}^{l}$ stands for blended image using $l-th$ level of Gaussian pyramid $G\{W\}_{ij,k}^{l}$ and $l-th$ level of Laplacian pyramid $\boldsymbol{L}\{I\}_{ij,k}^{l}$. K denotes the image and weight map quantity.

The diagram illustrating the flowchart of the proposed three-pass method shown in *Figure 1* illustrates the step-by-step process of the algorithm, which includes gamma correction, the use of different weight maps, and the fusion steps. The inputs and outputs of each pass are also depicted in the flowchart, showing how the output of the previous pass is used as the input for the subsequent pass.

The pseudo-code for the proposed algorithm is presented in *Table 1*. The pseudo-code serves as a high-level representation of the algorithmic steps and logic involved in the proposed research work. It provides a concise and structured methodology outline, enabling a better understanding of the algorithm's functioning and implementation.

3.1. Dataset For Dehazing

A major obstacle in evaluating dehazing techniques is the absence of clear images (known as "ground truth"), making it challenging to accurately measure the image's quality using both subjective and objective criteria. To address this issue, various datasets have been created, including FRIDA (Tarel et al., 2010) and FRIDA2 (Tarel et al., 2012), Middlebury (Scharstein et al., 2014), NYU v2 Kinect (Silberman et al., 2012), I-Haze (Ancuti et al., 2018a), O-Haze (Ancuti et al., 2018b), Dense Haze (Ancuti et al., 2019), HazeRD (Zhang et al., 2017), and RESIDE (Li et al., 2019), which contain ground truth images.

The dataset used in this study is the Reside-β version of the RESIDE dataset, which comprises of two subsets: the Outdoor Training Set (OTS) and the Real-world Task-Driven Testing Set (RTTS). The OTS subset comprises artificially hazed outdoor images along with a clear counterpart of them, while the RTTS subset contains real hazy outdoor images that do not have a corresponding clear version. These subsets are selected to provide diverse images for evaluating the image dehazing algorithm, including synthetic and real-world hazy images. The OTS subset allows for evaluating the visual appearance of the algorithm's output on a range of hazy and clear images. In contrast, the RTTS subset provides a more challenging test set of original hazy images representing real-world conditions.

Table 1. Pseudo-Code of Proposed Method

Algorithm 1: Single Image Haze Removal

Input: Hazy Image *I*
Result: Dehazed Image *J*
initialization;
Generate artificially under-exposed images by a set of gamma-correction on *I*;
for each *three artificially under-exposed images* **do**
    Calculate the DCP weight map for RGB color channels;
end
Apply image fusion to each artificially under-exposed image and weight map;
Generate artificially under-exposed images using the output image of the previous pass;
for each *three artificially under-exposed images* **do**
    Calculate the Saliency and Entropy weight maps for RGB color channels of the artificially under-exposed images and combine weight maps;
end
Apply image fusion to each artificially under-exposed image and weight map;
Apply Gray World and Illumination-Aware Color Correction Algorithm to the output image of the previous pass and use output of the second pass directly or CLAHE applied version as input;
for *each three input images* **do**
    Calculate the AlexNET and Contrast weight maps for RGB color channels of the input images and combine weight maps;
end
Apply image fusion to each artificially under-exposed image and weight map;
Obtain the final dehazed image *J* from the output of the third pass.

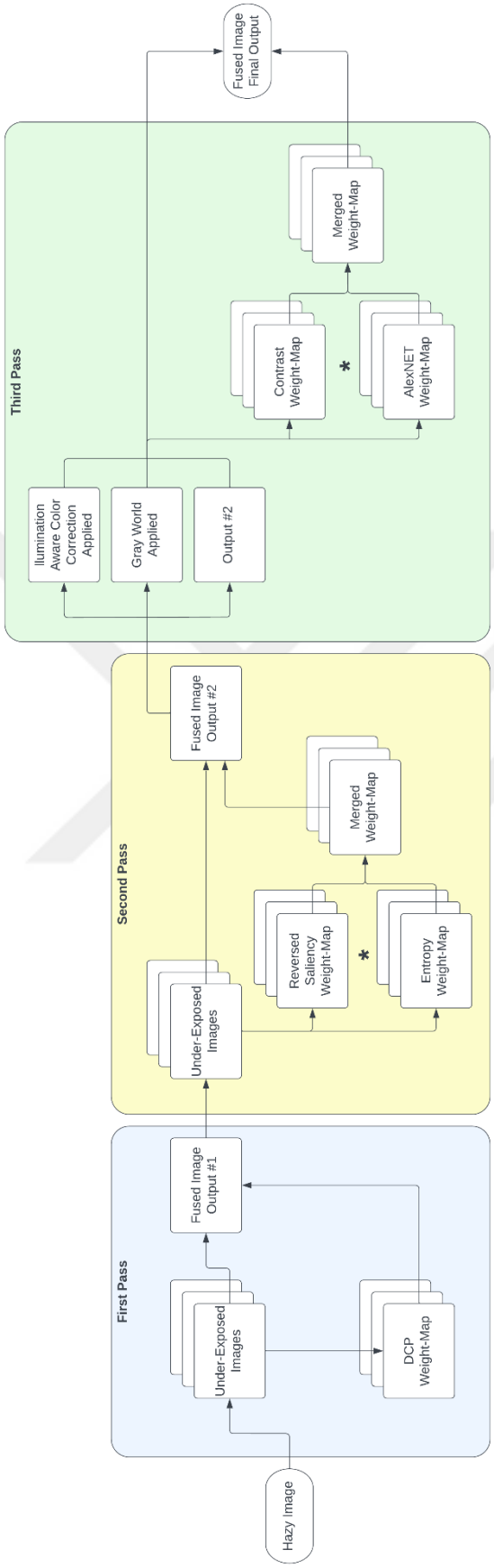

Figure 1. The flowchart of proposed dehazing algorithm.

3.2. Quality Assessment Methods

Image quality assessment (IQA) algorithms can be classified into three distinct groups based on the presence or absence of a ground-truth image: full-reference, reduced-reference, and no-reference methods (Wang and Yuan, 2017). The initial two categories necessitate the presence of a reference image, which can be a challenge in the case of image dehazing as it is often challenging to acquire a reference image depicting the identical scene without haze. Consequently, a no-reference evaluation technique is commonly employed; alternatively, a dehazed image can serve as a reference for evaluating the efficacy of algorithms.

In this study, two full-reference methods, PSNR and SSIM (Wang et al., 2004), and two no-reference methods, PIQE (Venkatanath et al., 2015), and BRISQUE (Mittal et al., 2012) are selected for IQA. However, as the main goal of the study is to enhance object detection performance, the average IQA scores may not fully reflect the success of the proposed algorithm. To address this, the contrast-limited adaptive histogram equalization (CLAHE) (Zuiderveld, 1994) technique is applied to the input of the third pass obtained from the second pass, resulting in better IQA scores for both full-reference and no-reference methods. The object detection algorithm YOLOv7 (Wang et al., 2022) is utilized to assess the aimed performance of the developed dehazing algorithm. YOLO (Redmon et al., 2016), an extensively employed object detection framework in computer vision research and applications, enables the efficient detection of objects within images through the subdivision of the input. Rectangles, accompanied by class labels and confidence scores, are assigned to the detected objects. By incorporating YOLOv7 into the evaluation process, the efficacy of the dehazing algorithm’s object detection performance can be successfully examined. YOLOv7 serves as a recognized and established benchmark for object detection tasks, rendering it a suitable choice for evaluating haze removal's impact on object detection performance.

3.3. Weight Maps

Enhancement methods that operate on the entire image at once are insufficient for improving the contrast of hazy scenes, since the haze's optical density varies across the image, leading to different effects on each pixel's values. In response to this limitation, Ancuti et al. (2013) suggested using various weight maps to address the issue. In their study, the effectiveness of employing a multi-scale fusion method for image dehazing is demonstrated. It has been shown that this approach efficiently removes haze from images by wisely selecting suitable weight maps and inputs.

In this study, five different weight maps are proposed: dark channel prior, saliency, entropy, contrast, and AlexNET network's $conv1$ layer weight maps. With these weight maps, information from hazy areas can be extracted from artificially underexposed input images.

Figure 2 visually represents the hazy input image and its corresponding three weight maps generated during the iterative dehazing process, ending in the final dehazed output. The weight maps depict the relevance and contribution of each pass in the dehazing algorithm. The progressive refinement of the weight maps suggests the iterative nature of the dehazing procedure. The hazy input image, weight maps, and the resulting dehazed image collectively provide an insightful visual demonstration of the efficacy of the proposed method.

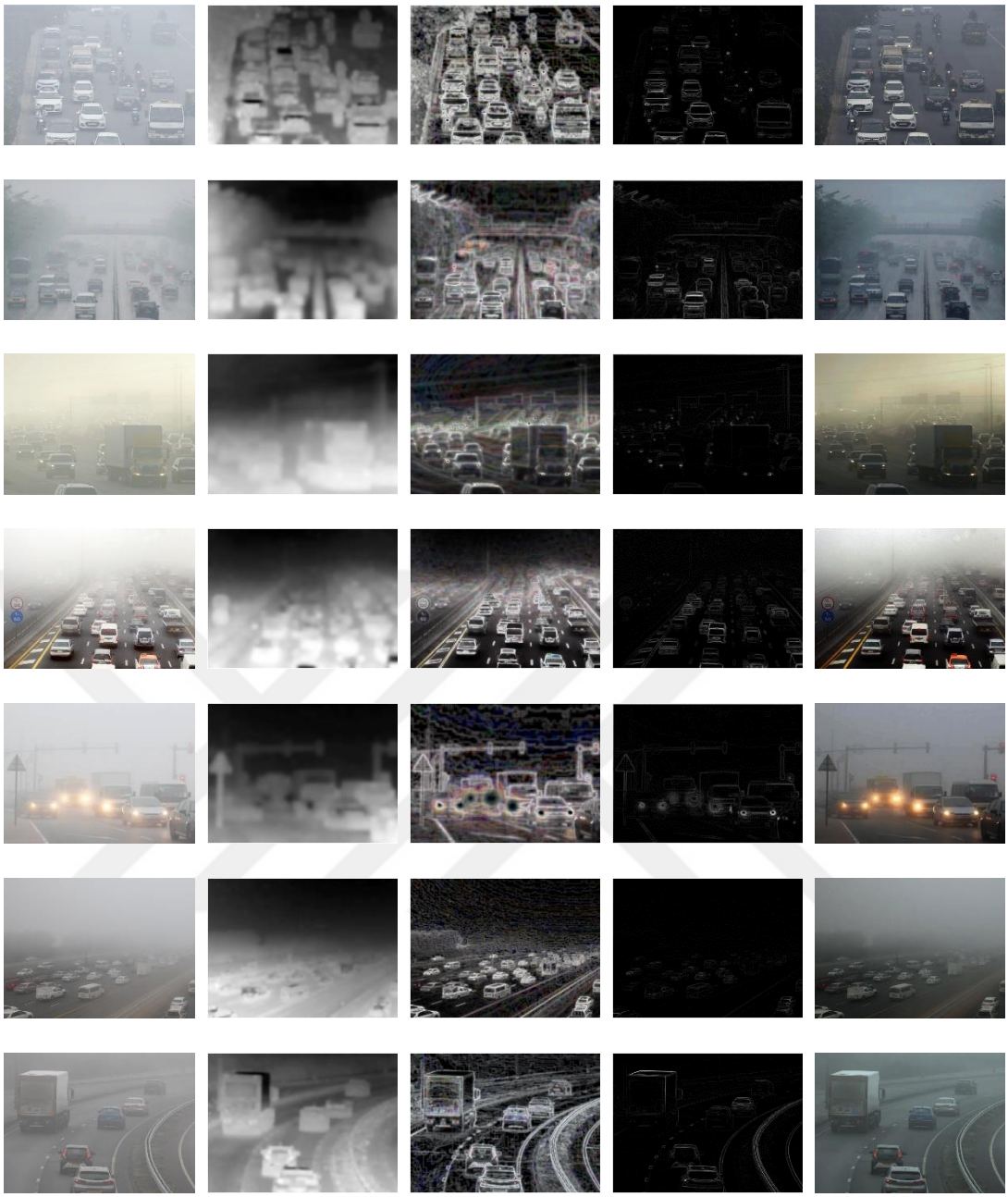

(a) (b) (c) (d) (e)

Figure 2. Hazy input image, weight maps (WM) of each pass and dehazed result of a real-world hazy image. (a) Hazy Input Image. (b) Weight Map of First Pass. (c) Weight Map of Second Pass. (d) Weight Map of Third Pass. (e) Dehazed Image.

3.3.1. Dark Channel Prior Weight Map

The dark channel prior (DCP) (He et al., 2009) is derived from a common feature observed in outdoor images that are free of haze. Specifically, many areas of the image that are not the sky exhibit pixels with particularly low levels of intensity in at least one color channel. This results in the minimum intensity of those areas being close to zero. DCP can be calculated using *Eq.(5):*

$$J^{dark}(x) = \min_{y \in \Omega(x)} \left(\min_{c \in \{r,g,b\}} J^c(y) \right) \quad (5)$$

where J^c refers to one of the color channels of image J, while Ω represents a local patch around point x in the image and y denotes the pixel in a local patch.

3.3.2. Saliency Weight Map

Saliency weight map (Ancuti et al., 2010) determines how noticeable an object or person is compared to the surroundings. This perceptual measurement of quality evaluates whether a particular object is distinct from other elements in the image or adjacent areas.

The saliency weight for input I_k is calculated pixel-wise using *Eq (6)*:

$$W_k^S(x) = ||I_k^{\omega_{hc}}(x) - I_k^{\mu}|| \quad (6)$$

where I_k^{μ} denotes the average pixel value of the $k-th$ input I_k, $I_k^{\omega_{hc}}$ represents the smoothed version of the same input and $W_k^S(x)$ represents the saliency weight.

3.3.3. Entropy Weight Map

Entropy weight map relies on the entropy of an image without haze being more significant compared to a hazy image taken at the identical scene because the haze-free image has a more random distribution than the hazy image (Park et al., 2014). Using the entropy weight map for image dehazing helps to preserve important details and edges in the image during the dehazing process. Entropy weight map (Gonzalez and Woods, 2018) is calculated using *Eq.(7):*

$$e(z) = -\sum_{i=0}^{L-1} p(z_i) \log_2 p(z_i) \quad (7)$$

where $e(z)$ denotes the entropy, z_i represents the intensity of L-level input and p represents the probability distribution of pixel intensities in the input. The entropy is calculated for each pixel in the image, resulting in an entropy map.

3.3.4. Contrast Weight Map

The topic of computing image gradients is conventional within the domain of image processing. Essentially, the magnitude of the gradient measures the degree of variation in the image, and areas with greater variation tend to have higher contrast, which corresponds to pixels with higher gradient magnitudes.

To generate the contrast weight map, the image undergoes two main steps. Firstly, a Gaussian filter with 5×5 box kernel is employed to perform image smoothing. Then, the image's gradient is computed in the x and y directions. The contrast weight map is obtained by calculating the magnitude of this gradient using *Eq.(8):*

$$W_n^C = \sqrt{(G_x)^2 + \left(G_y\right)^2} \quad (8)$$

where W_n^C represents the contrast WM of $n - th$ pass, G_x and G_y denotes the input image's partial derivatives along x and y spatial directions, respectively.

3.3.5. AlexNET Weight Map

Deep neural networks have demonstrated their efficacy to be highly successful in computer vision, particularly in image processing tasks, thanks to their ability to learn complex features from images. One notable example is AlexNET (Krizhevsky et al., 2012), which includes a powerful convolutional layer that can detect low-level features like edges and blobs. These features are critical in image dehazing, as they help to understand the structure of the scene. By using AlexNET's $conv1$ layer as a weight map in the third pass and applying in a log transformation, its contrast can be enhanced

and even more effective in dehazing. By using the resulting weight map, essential information about the scene's structure can be captured, making it a valuable addition to the other weight maps used in the algorithm.

The $conv1$ layer obtained from the input image of AlexNET, sized $227 \times 227 \times 3$, has dimensions of $55 \times 55 \times 96$. To select the most relevant WM, mutual information (MI) is employed to assess the correlation between the $conv1$ layer activations and an input image. MI measures the statistical dependence or correlation between two variables (Cover and Thomas, 2005). In this case, MI is evaluated between the $conv1$ layer's activations and the input image. A higher MI score indicates a stronger relationship between the $conv1$ layer activations and the input image.

3.4. Post-Processing Techniques

In addition to being used as post-processing techniques, Gray World and Illumination-Aware Color Correction algorithms are also used to create additional inputs for the third pass of the dehazing algorithm. The color temperature of the input images is normalized, and the color cast caused by haze is also eliminated using the illumination-aware color correction algorithm. The Gray World algorithm is used to adjust the color balance of the input images. These techniques are particularly effective in cases where the color cast caused by haze is severe. By using these algorithms to create additional inputs for the third pass, the algorithm is better able to gather specific object information and further improve the dehazing performance. This ensures that the final output is high quality and visually appealing to the end-users.

3.4.1. Gray World

The Gray World algorithm is a color balance correction method that aims to adjust the color balance of an image by scaling each color channel to have the same average value.

This algorithm's primary goal is to balance the color cast in a picture by assuming that the whole image's average color is approximated to be a shade of gray. The basic idea is to compute the mean value of each color channel before scaling the pixel values

within each channel by a factor that will make the mean value of that channel equal to a predefined alpha (α) value. This process is carried out individually for each channel to preserve the image's overall color balance.

In this algorithm, the alpha value is calculated dynamically. The normalized input image's mean intensity is used as an alpha value. This algorithm is calculated using the *Eq.(9):*

$$I'_{c_{r,g,b}}(x) = \frac{I_{c_{r,g,b}}(x)}{\overline{I_{c_{r,g,b}}}} \left(\frac{\overline{I_{c_r}} + \overline{I_{c_g}} + \overline{I_{c_b}}}{3} \right) \quad (9)$$

where $I'_{c_{r,g,b}}(x)$ denotes the corrected pixel value, $I_{c_{r,g,b}}(x)$ represents the original pixel value at position x in the image for each color channel RGB, $\overline{I_{c_{r,g,b}}}$ represents the average intensity value for each color channel RGB, and I_{c_r}, $\overline{I_{c_g}}$, and $\overline{I_{c_b}}$ represent average intensity of red, green, and blue channels, respectively.

3.4.2. Illumination-Aware Color Correction

The color correction algorithm adjusts the color balance of an image based on the statistics of the individual color channels (Kumar and Bhandari, 2020).

The color correction algorithm is applied using the *Eq.(10):*

$$\begin{aligned} I_{c_1 t}(x) = I_{c_1} &+ \frac{\alpha}{2}\left(\overline{I_{c_2}} - \overline{I_{c_1}}\right)\left(1 - I_{c_1}(x)\right) I_{c_2} \\ &+ \frac{\alpha}{2}\left(\overline{I_{c_3}} - \overline{I_{c_1}}\right)\left(1 - I_{c_1}(x)\right) I_{c_3} \end{aligned} \quad (10)$$

where $I_{c_1 t}(x)$ represents intensity value at position x of target c_1 color channel, $I_{c_1}(x)$ denotes intensity value at position x of the original image's c_1 color channel, $\overline{I_{c_1}}$, stands for the intensity value average of c_1 color channel, c_1, c_2, and c_3 corresponds to the RGB channels, and α denotes the illumination constant parameter varies between 0 and 1.

CHAPTER 4: EXPERIMENTAL RESULTS AND ANALYSIS

The experimental results and analysis section within this thesis encompasses the presentation of both quantitative and qualitative outcomes achieved by the proposed dehazing algorithm. The performance evaluation of the algorithm is conducted by employing various metrics, and a comparative analysis is conducted against numerous state-of-the-art methods. Through this comprehensive analysis, a perceptive examination of the strengths and weaknesses of the proposed approach is undertaken. Furthermore, insightful discussions are provided regarding potential avenues for future enhancements and advancements.

4.1. Computational Complexity Analysis

All experiments are performed on an Intel® Core™ i5-8250U CPU @ 1.60 GHz 4-core 8GB RAM machine using MATLAB R2022b. The suggested approach and all competing algorithms are used in their unmodified default configurations. The average execution time (Run-Time) of the algorithms in the comparison is given in *Table 2*. The highest score is shown in boldface.

Using parallel processing methods and implementing the algorithm in a language other than MATLAB may help reduce the computational complexity of the proposed algorithm. The simultaneous execution of several tasks is made possible by parallel processing, which can greatly increase the algorithm's overall speed and efficacy. The computational efficiency of the algorithm can also be increased by selecting a programming language tuned for performance and scalability, making it more appropriate for real-time and large-scale applications.

Table 2. The average execution time of the algorithms.

Methods	AMEF	CAP	DCP	MSCNN	Zhu et al.'s Method	Proposed Method
Run-Time (sec)	0.657	0.413	**0.123**	1.138	0.465	3.779

4.2. Comparison

To confirm the efficacy of the proposed dehazing algorithm, five methods are employed for comparison. Officially released codes of these methods are used for fair comparisons. Zhu's method (Zhu et al., 2021) and AMEF (Galdran, 2018) are used as fusion-based methods, while He et al.'s method (He et al., 2009) has utilized as a DCP-based method. Ren et al.'s MSCNN (Ren et al., 2016) has used as a deep learning-based method. Furthermore, the CAP method proposed by Zhu et al. (Qingsong Zhu et al., 2015) is also used for comparison purposes.

Due to the high performance of most dehazing algorithms in enhancing general outdoor images, the visual ranking of these algorithms can be challenging. To overcome this challenge, this thesis adopts a comprehensive evaluation framework. In addition to using the YOLOv7 object detection algorithm, various assessment methods are employed, including popular metrics such as PSNR and SSIM for full-reference evaluation, as well as PIQE and BRISQUE for no-reference evaluation. This combined approach enables a thorough evaluation that considers both subjective visual assessment and objective quality measures.

4.3. Test Images

To demonstrate object detection, a set of real hazy outdoor images captured under varying lighting conditions are selected from the RTTS dataset. Out of the 4322 images available, a diverse range of traffic-related scenes affected by haze are contained in the dataset. These images serve as representative samples to assess the performance of the object detection algorithm under various lighting and atmospheric conditions encountered in real-world scenarios. For image quality assessment, 520 artificially hazed outdoor images ($\beta = 0.2$ and $A = 0.9$) are selected from the OTS dataset with clear counterparts.

4.4. Object Detection Results

Figure *3* shows the YOLOv7 object detection algorithm results of all algorithms. Over-enhancement is significantly suffered by the result shown in Figure *3* (e) as the sky is

much darker and many artifacts exist. This is due to the problem of overestimating the transmission.

Despite its relatively lower visual quality, the primary goal of the proposed method is to enhance object detection performance, which it accomplishes by capturing numerous features. To improve the visual quality of the output, the proposed algorithm with the application of CLAHE can be utilized.

The object detection comparison of results clearly demonstrates the superior performance of the proposed method when compared to other state-of-the-art methods. As shown in *Figure 3*, the proposed method demonstrates superior performance compared to other existing methods. The proposed algorithm is able to detect more objects and fewer false positives compared to the other algorithms. This can be attributed to the unique combination of techniques used in the proposed algorithm, including a novel feature extraction method. Overall, these results imply that the proposed algorithm is a promising solution for object detection tasks in various real-world applications.

Figure 3. Comparison of several object identification techniques using the RTTS dataset real-world images. (a) The hazy images. (b) Hazy images' results. (c) AMEF results. (d) CAP results. (e) DCP results. (f) MSCNN results. (g) Zhu et al's results. (h) Proposed Algorithm's results.

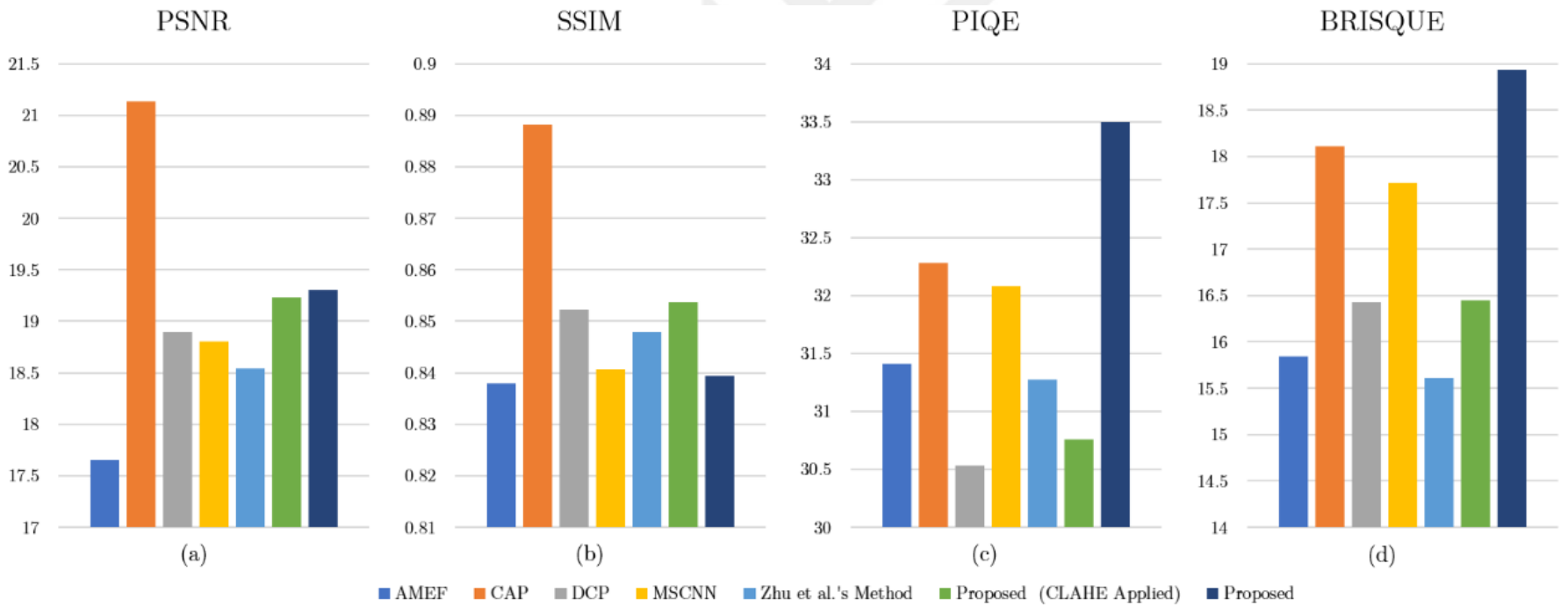

Figure 4. Objective evaluation comparison of six image dehazing methods on hazy images. (a) PSNR. (b) SSIM. (c) PIQE (d) BRISQUE.

4.5. Image Quality Assessment

Methods stated in *Section 3.2* are used over 520 artificially hazed outdoor images ($\beta = 0.2$ and $A = 0.9$) selected from the OTS dataset with clear counterparts. The average scores of stated methods are stated in *Table 3* and shown as graph in *Figure 4*. In *Table 3*, the worst scores are denoted in red, and the best two scores are highlighted bold-faced that draws attention to the methods that have achieved the highest scores, signifying their superior performance compared to the other methods.

Table 3. Quality Assessment Scores of Various Image Dehazing Methods.

Methods	PSNR	SSIM	PIQE	BRISQUE
AMEF	17.65	0.84	31.41	15.85
CAP	**21.13**	**0.89**	32.28	18.11
DCP	18.90	0.85	**30.53**	**16.43**
MSCNN	18.80	0.84	32.08	17.72
Zhu et al.'s Method	18.54	0.85	31.27	**15.61**
Proposed	19.30	0.84	33.50	18.93
Proposed (CLAHE Applied)	**19.23**	**0.85**	**30.76**	16.44

To assess the ability of image dehazing algorithms to keep the structural information of the images, the structural similarity index (SSIM) is commonly used. A high SSIM value indicates a high similarity between ground truth and dehazed images, while a low SSIM value indicates the contrary. Peak signal-to-noise ratio (PSNR), widely employed to quantify the efficacy of image dehazing algorithms, is another important index for assessing image quality. A higher PSNR value implies a stronger resemblance within the ground truth and dehazed images, indicating better image quality. Conversely, a lower PSNR value implies a greater discrepancy within the ground truth and dehazed images, indicating lower image quality. Therefore, PSNR is a crucial metric to assess the accuracy of image dehazing algorithms.

The performance of different image-dehazing algorithms, including AMEF, CAP, DCP, MSCNN, and Zhu et al.'s method, the proposed algorithm, and the proposed algorithm with CLAHE are evaluated. Evaluation is based on four metrics: PSNR, SSIM, PIQE, and BRISQUE. Among the tested algorithms, CAP achieved the highest results in PSNR and SSIM, while the proposed algorithm (CLAHE applied) ranked second in PSNR and SSIM statistics.

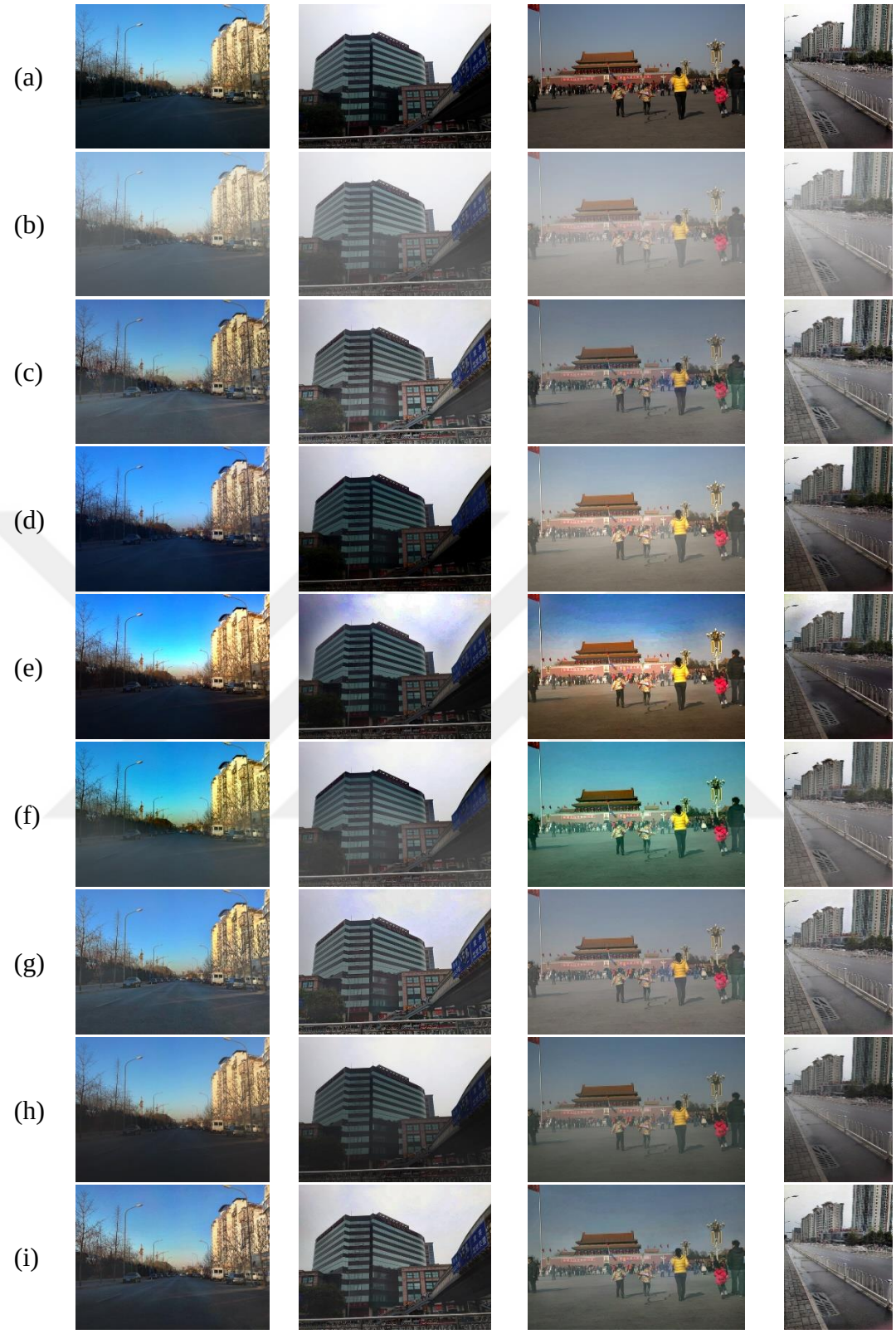

Figure 5. Qualitative comparison of various techniques on OTS subset synthetically hazed images. (a) Clear Image. (b) Hazy images ($\beta = 0.2$ and $A = 0.9$). (c) AMEF results. (d) CAP results. (e) DCP results. (f) MSCNN results. (g) Zhu et al's results. (h) Proposed Algorithm's results. (i) Proposed Algorithm with CLAHE results.

However, in terms of PIQE and BRISQUE, CAP produced relatively high scores, indicating inferior results compared to the other algorithms. Among all algorithms, the proposed algorithm (CLAHE applied) achieved a better score in PIQE and a moderate score in BRISQUE, demonstrating its superiority and robustness in producing well-dehazed images with few artifacts and distortion.

Overall, the proposed algorithm with CLAHE applied shows the most balanced performance, outperforming or matching the state-of-the-art algorithms across all metrics. The qualitative comparison of five state-of-the-art dehazing methods' outputs is demonstrated in *Figure 5*.

CHAPTER 5: CONCLUSION

In this study, a novel image dehazing algorithm that utilizes deep learning features and fusion techniques is presented. The effectiveness of the proposed method, which outperforms cutting-edge object identification systems, is demonstrated through comprehensive experiments on benchmark datasets.

The proposed method comprises of a multi-pass image dehazing stage, followed by a fusion process. By using multiple passes of image dehazing, haze is removed successfully, and the visibility of objects is enhanced, resulting in improved object detection efficacy. The fusion part can combine details from different feature maps extracted at various scales, enabling the capture of both local and global contextual information for object detection.

Furthermore, the impact of various parameters on the efficiency of the proposed method is investigated through experiments. Experimental results show that the choice of fusion method and the number of dehazing passes significantly affect the final detection superiority.

The proposed algorithm can be further improved by incorporating additional contextual information, such as scene semantics and object relationships. Additionally, investigating the applicability of the proposed algorithm to other tasks within the realm of computer vision, including semantic segmentation and instance segmentation, can be a future research direction.

The algorithm being proposed could greatly enhance the efficacy of detecting objects in hazy environments. This advancement would have significant benefits for a variety of real-world use cases, including autonomous driving, surveillance, and robotics.

REFERENCES

Agrawal, S.C. and Jalal, A.S. (2022) *A Comprehensive Review on Analysis and Implementation of Recent Image Dehazing Methods,* Archives of Computational Methods in Engineering, vol. 29, pp. 4799–4850.

Ancuti, C.O. and Ancuti, C. (2013) *Single Image Dehazing by Multi-Scale Fusion,* IEEE Transactions on Image Processing, vol. 22, pp. 3271–3282.

Ancuti, C.O., Ancuti, C. and Bekaert, P. (2010) *Effective single image dehazing by fusion*, IEEE International Conference on Image Processing (ICIP 2010), Hong Kong, pp. 3541–3544.

Ancuti, C.O., Ancuti, C., Sbert, M. and Timofte, R. (2019) *Dense-Haze: A Benchmark for Image Dehazing with Dense-Haze and Haze-Free Images*, 2019 IEEE International Conference on Image Processing (ICIP), Taipei, Taiwan, pp. 1014–1018.

Ancuti, C.O., Ancuti, C., Timofte, R. and De Vleeschouwer, C. (2018a) *I-HAZE: A dehazing benchmark with real hazy and haze-free indoor images*, 2018 Advanced Concepts for Intelligent Vision Systems (ACIVS), Lecture Notes in Computer Science, vol 11182, Springer, Cham.

Ancuti, C.O., Ancuti, C., Timofte, R. and De Vleeschouwer, C. (2018b) *O-HAZE: A Dehazing Benchmark with Real Hazy and Haze-Free Outdoor Images,* 2018 IEEE/CVF Conference on Computer Vision and Pattern Recognition Workshops (CVPRW), Salt Lake City, UT, pp. 867–8678.

Burt, P. and Adelson, E. (1983) *The Laplacian Pyramid as a Compact Image Code*, IEEE Transactions on Communications, vol 31, pp. 532–540.

Cai, B., Xu, X., Jia, K., Qing, C. and Tao, D. (2016) *DehazeNet: An End-to-End System for Single Image Haze Removal*, IEEE Transactions on Image Processing, vol. 25, 5187–5198.

Cover, T.M. and Thomas, J.A. (2005) *Entropy, Relative Entropy, and Mutual Information*, 2nd Edition, *Elements of Information Theory*, pp. 13–55.

Fattal, R. (2008) *Single image dehazing*, ACM Transactions on Graphics, 27, 1–9.

Fu, X., Wang, J., Zeng, D., Huang, Y. and Ding, X. (2015) *Remote Sensing Image Enhancement Using Regularized-Histogram Equalization and DCT*, IEEE Geoscience and Remote Sensing Letters, vol. 12, pp. 2301–2305.

Galdran, A. (2018) *Image dehazing by artificial multiple-exposure image fusion*, Signal Processing, vol 149, pp. 135–147.

Gonzalez, R.C. and Woods, R.E. (2018) *Digital image processing*, 4th Edition, New York: Pearson.

Harish Babu, G. and Venkatram, N. (2020) *A survey on analysis and implementation of state-of-the-art haze removal techniques,* Journal of Visual Communication and Image Representation, vol. 72, 102912.

He, K., Sun J. and Tang, X. (2009) *Single image haze removal using dark channel prior,* 2009 IEEE Conference on Computer Vision and Pattern Recognition. (CVPR Workshops), Miami, FL, pp. 1956–1963.

He, S., Yang, Q., Lau, R.W.H. and Yang, M.-H. (2016) *Fast Weighted Histograms for Bilateral Filtering and Nearest Neighbor Searching*, IEEE Transactions on Circuits and Systems for Video Technology, vol. 26, pp. 891–902.

Krizhevsky, A., Sutskever, I. and Hinton, G.E. (2012) *ImageNet Classification with Deep Convolutional Neural Networks*, in Pereira, F., Burges, C.J., Bottou, L., Weinberger, K.Q. (eds.) *Advances in Neural Information Processing Systems,* Curran Associates, Inc., vol. 5.

Kumar, M. and Bhandari, A.K. (2020) *Contrast Enhancement Using Novel White Balancing Parameter Optimization for Perceptually Invisible Images*, IEEE Transactions on Image Processing, vol. 29, pp. 7525–7536.

Li, B., Peng, X., Wang, Z., Xu, J. and Feng, D. (2017) *AOD-Net: All-in-One Dehazing Network*, 2017 IEEE International Conference on Computer Vision (ICCV), Venice, pp. 4780–4788.

Li, B., Ren, W., Fu, D., Tao, D., Feng, D., Zeng, W. and Wang, Z. (2019) *Benchmarking Single-Image Dehazing and Beyond*, IEEE Transactions on Image Processing, vol. 28, pp. 492–505.

Li, Z., Zheng, J., Zhu, Z., Yao, W. and Wu, S. (2015) *Weighted Guided Image Filtering*, IEEE Transactions on Image Processing, vol. 24, pp. 120–129.

Mertens, T., Kautz, J. and Van Reeth, F. (2007) *Exposure Fusion*, 15th Pacific Conference on Computer Graphics and Applications (PG'07), Maui, HI, pp. 382–390.

Mittal, A., Moorthy, A.K. and Bovik, A.C. (2012) *No-Reference Image Quality Assessment in the Spatial Domain*, IEEE Transactions on Image Processing, vol. 21, pp. 4695–4708.

Park, D., Park, H., Han, D.K. and Ko, H. (2014) *Single image dehazing with image entropy and information fidelity*, 2014 IEEE International Conference on Image Processing (ICIP), Paris, France, pp. 4037–4041.

Qiu, Y., Lu, Y., Wang, Y. and Jiang, H. (2023) *IDOD-YOLOV7: Image-Dehazing YOLOV7 for Object Detection in Low-Light Foggy Traffic Environments*, Sensors, vol. 23, 1347.

Redmon, J., Divvala, S., Girshick, R. and Farhadi, A. (2016) *You Only Look Once: Unified, Real-Time Object Detection*, IEEE Conference on Computer Vision and Pattern Recognition, Las Vegas, pp. 779-788.

Ren, W., Liu, S., Zhang, H., Pan, J., Cao, X. and Yang, M.-H. (2016) *Single Image Dehazing via Multi-scale Convolutional Neural Networks*, in Leibe, B., Matas, J., Sebe, N., Welling, M. (eds.) *Computer Vision – ECCV 2016*, Lecture Notes in Computer Science. Springer International Publishing, Cham, pp. 154–169.

Scharstein, D., Hirschmüller, H., Kitajima, Y., Krathwohl, G., Nešić, N., Wang, X. and Westling, P. (2014) *High-Resolution Stereo Datasets with Subpixel-Accurate Ground Truth*, in Jiang, X., Hornegger, J., Koch, R. (eds.) *Pattern Recognition*, Lecture Notes in Computer Science. Springer International Publishing, Cham, pp. 31–42.

Silberman, N., Hoiem, D., Kohli, P. and Fergus, R. (2012) *Indoor Segmentation and Support Inference from RGBD Images*, in Fitzgibbon, A., Lazebnik, S., Perona, P., Sato, Y., Schmid, C. (eds.) *Computer Vision – ECCV 2012*, Lecture Notes in Computer Science. Springer Berlin Heidelberg, Berlin, Heidelberg, pp. 746–760.

Sun, W., Wang, H., Sun, C., Guo, B., Jia, W. and Sun, M. (2015) *Fast single image haze removal via local atmospheric light veil estimation*, Computers & Electrical Engineering, vol. 46, 371–383.

Tan, R.T. (2008) *Visibility in bad weather from a single image*, 2008 IEEE Conference on Computer Vision and Pattern Recognition (CVPR), Anchorage, AK, USA, pp. 1–8.

Tarel, J.-P., Hautiere, N., Caraffa, L., Cord, A., Halmaoui, H. and Gruyer, D. (2012) *Vision Enhancement in Homogeneous and Heterogeneous Fog*, IEEE Intelligent Transportation Systems Magazine, vol. 4, pp. 6–20.

Tarel, J.-P., Hautiere, N., Cord, A., Gruyer, D. and Halmaoui, H. (2010) *Improved visibility of road scene images under heterogeneous fog*, 2010 IEEE Intelligent Vehicles Symposium (IV), La Jolla, CA, USA, pp. 478–485.

Venkatanath, N., Praneeth, D., Maruthi Chandrasekhar Bh, Channappayya, S.S., and Medasani, S.S. (2015) *Blind image quality evaluation using perception based features*, 2015 Twenty First National Conference on Communications (NCC), Mumbai, India, pp. 1–6.

Wang, C.-Y., Bochkovskiy, A. and Liao, H.-Y.M. (2023) *YOLOv7: Trainable bag-of-freebies sets new state-of-the-art for real-time object detectors*, Proceedings of the IEEE/CVF Conference on Computer Vision and Pattern Recognition (CVPR), pp. 7464-7475.

Wang, J., Lu, K., Xue, J., He, N. and Shao, L. (2018) *Single Image Dehazing Based on the Physical Model and MSRCR Algorithm*, IEEE Transactions on Circuits and Systems for Video Technology, vol. 28, pp. 2190–2199.

Wang, W. and Yuan, X. (2017) *Recent advances in image dehazing*, IEEE/CAA J. Autom. Sinica, vol. 4, pp. 410–436.

Wang, Z., Bovik, A.C., Sheikh, H.R. and Simoncelli, E.P. (2004) *Image Quality Assessment: From Error Visibility to Structural Similarity*, IEEE Transactions on Image Processing, vol. 13, 600–612.

Zhang, Y., Ding, L. and Sharma, G. (2017) *HazeRD: An outdoor scene dataset and benchmark for single image dehazing*, 2017 IEEE International Conference on Image Processing (ICIP), Beijing, pp. 3205–3209.

Zhang, Y.-Q., Ding, Y., Xiao, J.-S., Liu, J. and Guo, Z. (2012) *Visibility enhancement using an image filtering approach*, EURASIP Journal on Advances in Signal Processing, 220.

Zhu, Q., Mai, J. and Shao, L. (2015) *A Fast Single Image Haze Removal Algorithm Using Color Attenuation Prior*, IEEE Transactions on Image Processing, vol. 24, pp. 3522–3533.

Zhu, Z., Wei, H., Hu, G., Li, Y., Qi, G., and Mazur, N. (2021) *A Novel Fast Single Image Dehazing Algorithm Based on Artificial Multiexposure Image Fusion*, IEEE Transactions on Instrumentation and Measurement, vol. 70, pp. 1–23.

Zuiderveld, K. (1994) *Contrast Limited Adaptive Histogram Equalization*, Graphics Gems, Elsevier, pp. 474–485.